

Point-contact spectroscopy of MgB_2 P. Samuely,¹ P. Szabo,¹ J. Kacmarčík,¹ T. Klein,² A. G. M. Jansen³¹ Institute of Experimental Physics, Slovak Academy of Sciences, Watsonova 47, SK-043 53 Kosice, Slovakia.² Université Joseph Fourier, BP 53, F-38041 Grenoble Cedex 9, France.³ Grenoble High Magnetic Field Laboratory, MPI-FKF and CNRS, F-38042 Grenoble, France.

(March 22, 2024)

Point-contact spectroscopy measurements on magnesium diboride reveal the existence of two superconducting energy gaps closing at the same transition temperature in line with the multiband model of superconductivity. The sizes of the two gaps ($\Delta_1 = 2.8$ meV and $\Delta_2 = 6.5$ –7 meV) are respectively smaller and larger than the expected weak coupling value of the one-gap superconductor. The smaller gap is rapidly closed by a small magnetic field of about 1–2 Tesla much lower than the real upper critical field H_{c2} . The larger gap is closed at the anisotropic H_{c2} . Above the gap energies reproducible non-linearities are observed at the characteristic phonon energies of MgB_2 .

PACS numbers: 74.50.+r, 74.60.Ec, 74.72.-h

I. INTRODUCTION

Point-contact spectroscopy offers the possibility to study very fundamental superconducting properties. Namely, the superconducting energy gap can be addressed via the Andreev reflection and the electron-phonon (boson) interaction can be inferred as well. From the very beginning since the discovery of MgB_2 [1] this technique has been applied for the investigation of this compound. Here, we shortly review the state of art which unequivocally supports the fact that MgB_2 represents an extraordinary example of multigap superconductivity which phenomenon attracts interest since the fifties [2,3].

The electronic structure calculations have predicted [4] that several electronic bands cross the Fermi level in MgB_2 with two different superconducting gaps at different sheets. These predictions have been experimentally evidenced by different techniques like specific heat measurements [5], tunneling [6,8], Raman spectroscopy [9], and so on. Among these investigation methods also spectroscopy based on the Andreev reflection process gave one of the proofs of such multigap superconductivity [10]. For the larger gap attributed to the two-dimensional σ -band parallel to the c -axis originating from the boron $p_{x,y}$ orbitals, the reduced gap value $2\Delta_2/k_B T_c \approx 4$ has been found. The smaller gap on the 3D π -band of the boron p_z -orbitals has the reduced value much below the BCS weak coupling limit of a one-band superconductor ($2\Delta_1/k_B T_c \approx 1.7$). The behavior of the both gaps in magnetic field has been studied in detail [10,12]. The small gap is closed very rapidly by a small field of about 1–2 Tesla at low temperatures. The large gap is closed at the real upper critical field of MgB_2 which is anisotropic.

The relatively high value of the superconducting crit-

ical temperature T_c in MgB_2 is supposed to originate from the strong anharmonic coupling of the σ -band to the E_{2g} phonons [4]. The recent de Haas-van Alphen experiments [13] give indications for such an anisotropic electron-phonon interaction, but there is no direct spectroscopic evidence for the overall shape of the Eliashberg function of the electron-phonon interaction. The very first point-contact spectroscopy studies of the electron-phonon interaction which are available [14,17] indicate reproducible non-linearities of the current-voltage characteristics at the MgB_2 characteristic phonon energies. Further experiments and theoretical studies are necessary to elucidate details of the phononic interaction mechanism.

II. SUPERCONDUCTING ENERGY GAPS

Below T_c a phase coherent state of Cooper pairs is formed in a superconductor. Transport of charge carriers across a normal metal/superconductor (N/S) interface involves the unique process of Andreev reflection. If the N/S interface consists of a ballistic point contact with the mean free path l bigger than the diameter of the contact orifice, the excitation energy eV of charge carriers is controlled by the applied voltage V . For a quasiparticle incident on the N/S interface with an excitation energy $eV < \Delta$, a direct transfer of the charge carriers is forbidden because of the existence of the energy gap in the quasiparticle spectrum of the superconductor. For this case, the charge transfer of an injected charge carrier takes place via the retroreflection of a hole back into the normal metal with the formation of a Cooper pair in the superconductor. At excitation energies above the

gap quasiparticles can be transferred directly across the interface. The Andreev reflection process leads to a two times higher conductance of a N/S contact at $V < \approx e$ (zero-temperature limit) for the case of ballistic transport with transmission probability of the charge carriers $T = 1$. The opposite limit of ballistic transport is given by the tunneling process for an insulating barrier at the interface where $T \ll 1$. For Gievert tunneling between a superconductor and a normal metal, it is well known that the conductance goes to zero for $eV < \Delta$ (again in the zero-temperature limit). In contrast to the point-contact tunneling where the well-developed gap structures could also be due to other effects, like small particle charging [18], the Andreev reflection directly probes the coherent superconducting state. The more general case for arbitrary transmission T has been treated by Blonder, Tinkham and Klapwijk (BTK) [19]. The voltage dependence of the conductance of a N/S contact gives direct spectroscopic information on the superconducting order parameter. The conductance data can be compared with the BTK theory using as input parameters the energy gap Δ , the parameter Z (measure for the strength of the interface barrier with transmission coefficient $T = 1/(1+Z^2)$ in the normal state), and a parameter Γ for the quasiparticle lifetime broadening [20]. The evolution of the $dI=dV$ vs. V curves for different interfaces characterized with the barrier strength Z is schematically presented in Fig. 1a.

The first point-contact measurements on sintered MgB_2 pellets were performed by Schmidt et al. [21]. They showed that by the Au tip it was possible to change from the Gievert tunneling regime to the pure Andreev reflection. In both cases the s-wave gap was observed with a value of 4.3 meV. The smallness of this value compared to the expected value for a 39-K BCS superconductor was ascribed to a chemically modified surface layer with lower T_c , but the particular T_c of the point contact was not determined.

Kohen and Deutschler [22] found the energy gap in the polycrystalline MgB_2 scattered between 3 and 4 meV. The point contacts were done by means of the Au tip. The temperature dependence of the 3 meV energy gap followed the BCS form with T_c about 29 K. But even for this transition temperature, reduced in comparison with the bulk material, the resulting $2\Delta/k_B T_c \approx 2.4$ is much too small for a weak coupling BCS superconductor. The Fermi velocity $4.7 \cdot 10^7$ cm/s was calculated from the Z parameter with an assumption that the lowest Z originated just from the Fermi velocity mismatch between Au and MgB_2 . The obtained value was in agreement with the band structure calculations [23].

Measurements by Plecenik et al. [24] on MgB_2/Ag and MgB_2/In junctions performed on MgB_2 wires indicated the same problem with a small size of the energy gap. The temperature dependence of the 4 meV energy gap showed a significant deviation from the BCS form which

has been ascribed to an interference of two gaps with two different T_c 's in line with the published multigap scenario [4]. In their model Liu et al. [4] suggested that the two gaps are sensitive to impurity scattering. In contrast to Anderson's theorem for a one-gap superconductor, non-magnetic interband scattering can decrease T_c in this case of multigap superconductivity. Moreover, in the limit of strong scattering both gaps will be averaged into one single BCS gap ($\Delta \approx 4$ meV) which will close at $T_c \approx 27$ K. Plecenik et al. suggested that their point contacts represent a parallel connection of two junctions: one probing the small gap in the clean region and another the averaged BCS gap in the dirty part with a reduced T_c .

Laube et al. [25] and Gonnelli et al. [26] have also proposed explanations for the observed small gaps in their data in terms of multigap superconductivity.

Indications for the two-gap superconductivity have been found in the point-contact measurements of S. Lee et al. [27] and Li et al. [28]. The latter group claim the second large gap being around 10 meV which is much higher than the other experimental observations and the theoretical predictions.

In our work [10] we have shown the presence of two superconducting energy gaps in MgB_2 closing at the same bulk T_c . The point-contact measurements have been performed on polycrystalline MgB_2 samples with critical temperature $T_c = 39.3$ K and width $T_c = 0.6$ K of the superconducting transition. The pressure-type contacts could be adjusted in-situ by pressing a copper tip on the freshly polished surface of the MgB_2 superconductor using a differential screw mechanism. The crystallites of the MgB_2 samples were larger than a few micron. For a typical size of the metallic constriction below 10 nm, the point-contact probes therefore presumably a single crystallite but of unknown orientation.

In figure 2 we show typical examples of the differential conductance $dI=dV$ versus voltage spectra for Cu- MgB_2 point contacts in the superconducting state at 4.2 K. The three upper curves reveal a clear two-gap structure corresponding to the maxima placed symmetrically around zero bias. However, 90% of the contacts reveal a spectrum dominantly showing the small-gap structure with only a small shoulder-like contribution around the large-gap voltage. These variations from contact to contact are ascribed to current injection along different crystal directions of locally probed crystallites. The conductance curves of figure 2 have been fitted to the BTK theory using the sum of two contributions, $G_{BTK} + (1 - \alpha) G_{BTK}$, with a weight factor α between the small- and large-gap contributions, and α respectively. Details of the fitting to the sum of two BTK conductances are shown in Fig. 1b. The weight factor varied from 0.65 to 0.95 for the different contacts. The resulting energy gaps are $\Delta_{small} = 2.8 \pm 0.1$ meV for the small gap and $\Delta_{large} = 6.8 \pm 0.3$ meV for the large gap.

Point-contact data with a very low peak(s) height to background ratio (PHBR) have been reported in some of the above mentioned papers. In the case of the (prevailing) one-gap spectrum the low PHBR (e.g. in comparison with those in Fig. 1a) is caused by the large smearing parameter Γ . But even a structureless, parallel leakage current to the normal regions on the surface of MgB₂ can occur as mentioned in [24]. In the case of an important contribution of the both conductances to the spectrum (we have found $\Gamma = 0.65$) with generally two different broadenings and Z parameters, PHBR is more complicated but for a low T_c it never went below 1.4 in our measurements. The spectra shown in Fig. 2 reveals also the lowered PHBR in comparison with those the Fig. 1b and Fig. 3. Again, it is caused by the increased broadening parameter. For example $\Gamma = 0.13$ and $\Gamma = 0.07$ is found for the top curve and $\Gamma = 0.22$ in the case of the bottom curve.

In the calculations of two-band superconductivity in MgB₂ [4], the small gap is situated on the isotropic band and the large gap on the two-dimensional band (cylindrically shaped parallel to the c -axis). The Fermi surface topology of the two bands would explain the observed differences in the spectra for different contact orientations. The small gap, being isotropic, will be observed for all directions of current injection. However, the two-dimensional cylindrical Fermi surface will give most contribution to the interface current for current injection parallel to the ab -plane. The observation of two-gap structures in a minority of the investigated contacts might mean that the crystallites in the polycrystalline samples are mostly textured with the ab -planes at the surface. Thus, the spectra in Fig. 2 represent an evolution from the c -axis tunneling to the ab -band (bottom curve) to the bigger ab -plane contributions (higher curves) revealing the both ab - and c -gaps.

The smaller gap could a priori be caused by different reasons, including a surface layer of reduced superconductivity or surface proximity effects. However, most of the scenarios would still require a scaling of the gap with the critical temperature. That is why it was important to show an existence of the small gap at high temperatures in order to establish its origin in the two-band superconductivity. The temperature dependencies of the point-contact spectra have been examined on different samples. Due to thermal smearing, the two well resolved peaks in the spectrum merge together as the temperature increases. Consequently, the presence of two gaps is not so evident in the raw data (see Fig. 3a). For instance at 25 K the spectrum is reduced to one smeared maximum around zero bias. Such a spectrum itself could be fitted by the BTK formula with only one gap, but the transparency coefficient Z would have to change significantly in comparison with the lower temperatures and moreover a large smearing factor Γ would have to be introduced. However our data could be well fitted at all

temperatures by the sum of two BTK contributions with the transparency coefficient Z and the weight factor kept constant and without any parallel leakage conductance. The point-contact conductances of one spectrum at different temperatures are shown in Fig. 3a together with the corresponding BTK fits. The resulting energy gaps Δ_1 and Δ_2 together with those obtained for two other point contacts with different weight values are shown in Fig. 3b. In a classical BCS theory, an energy gap with $\Delta = 2.8$ meV could not exist for a system with T_c above $2.35k_B T_c = 19$ K, but as shown in Ref. [29] even a one-gap spectrum (shown as the bottom curve in Fig. 2) leads to the same temperature dependence $\Delta(T)$ with the bulk T_c as those indicated in Fig. 3b.

Since it is evident that both gaps are closing near the same bulk transition temperature, our data give experimental support for the two-gap model. We obtained a very weakly coupled gap with $2\Delta = k_B T_c \cdot 1.7$ and a strongly coupled gap with $2\Delta = k_B T_c \cdot 4$ in very good agreement with the predictions of Brinkman et al. [30] (a 3D gap ratio $2\Delta = k_B T_c \cdot 1.61$ and a 2D gap ratio $2\Delta = k_B T_c \cdot 4.22$). The temperature dependencies are in a good agreement with the prediction of the BCS theory. Small deviations from this theory have been predicted by Liu et al. but these deviations are within our error bars for the large gap while in the case of the small gap there is a tendency for more rapid closing at higher temperatures near to T_c (see Fig. 3b) as expected theoretically.

Later point-contact measurements confirmed the two-gap scenario in MgB₂. Bugoslavsky et al. [31] have demonstrated in their point contacts made on MgB₂ c -oriented thin films that the two distinct gaps can be evidenced already in the raw data at low temperatures ($\Delta_1 = 2.3$ meV and $\Delta_2 = 6.5$ meV) and they both close at the same bulk T_c . The observed differences in relative weight of the two gaps have also been ascribed to differences in crystallographic orientation under the Au tip and in barrier strength of their junctions. Bobrov et al. [14] and Naidyuk et al. [32] have presented the Andreev reflection spectra on the Ag/MgB₂ c -axis oriented 110 point contacts at 4.2 K. Their histogram of the gap distribution reveals distinct maxima at 2.4 and 7 meV.

Very recently Gonnelli et al. [33] have presented the point-contact spectroscopy on the MgB₂ single crystals. Their directional measurements have shown that the point-contact current parallel to the MgB₂ ab -plane probes both the ab and c bands revealing the two gaps ($\Delta_1 = 7.1$ meV and $\Delta_2 = 2.9$ meV) while the point-contact current injected along the c -axis reveals only one gap on the c -band. They also confirmed that the temperature dependence of the small gap reveals a stronger suppression near T_c while the large gap closes in line with the BCS temperature dependence.

Figure 4 demonstrates that the application of a magnetic field has been important to show the co-presence

of both small and large energy gap at high temperatures much above the temperature $T_c = 2.352k_B^{-1} \approx 19$ K corresponding to the BCS weak coupling limit. Indeed, the two distinct gaps clearly visible in the Andreev reflection spectrum at low temperatures get completely merged together due to thermal smearing at temperatures above 20 K. However, because the small gap is very sensitive to the applied field, the large-gap spectrum becomes better resolved in a field of a few tenths of Tesla even at temperatures above 30 K. The suppression of the small gap structure enhances the large-gap structure which is only suppressed at larger fields. This difference in the field sensitivity of both gaps published for the first time in our previous paper [10] opened the question about different magnetic field scales in the separate σ and π bands.

III. UPPER CRITICAL MAGNETIC FIELDS

Fig. 5 shows the behavior of the junction with the prevailing one-gap spectrum (weight factor of 0.95 of the π -band contribution) as a function of magnetic field at 4.2, 15 and 25 K. The effect of the applied magnetic field is very unexpected. The small magnetic fields below 2 T first shift the peak position to higher voltages. In the usual case of a one-gap superconductor the application of magnetic field can only lead to a shrinkage of the distance between the gap-like peaks in the point-contact/tunneling spectrum [34]. This is a simple consequence of the fact that the magnetic pair-breaking for increasing applied field fills up forbidden states inside the gap. Obviously, the effect demonstrated in Fig. 5 is due to an interplay of the two gaps which are inevitably always present together in any spectrum with arbitrary weight factor. As calculated by Brinkman et al. [30] even for strictly c -axis tunneling there is one percent tunneling probability into the π -band. However, unlike the case of tunneling spectroscopy with a very dominant contribution for perpendicular-to-the-barrier transport, we have to note that the ballistic transport in metallic contacts injects electrons through the contact with a much larger \cos -angular spreading. Thus, if in some cases only a peak due to the smaller gap is apparent, its width is hiding a contribution of the second gap. Then, in a magnetic field, the small gap in the π -band is rapidly suppressed and the large gap will definitely emerge. This superposition of the rapidly suppressing peak of the small gap and the emerging of the large one with a very small weight factor causes the observed shift of the peak towards higher voltages. At even higher fields the magnetic pair-breaking in the π -band leads to conventional shrinkage of the broadened gap peaks of the large gap. Such a smooth shift without any major change in peak position during transition from prevailing observation of the small gap to the large one is a consequence of an important broadening already at zero magnetic field. With

magnetic field the broadening substantially increases and the two "peaks" merge to the one. Fig. 4 demonstrates the effect of the field on the spectrum with a small broadening at zero field. At 4.2 K the two peaks or shoulders from the large and small gaps are well separated and they just shrink their voltage position with a field. At 20 K the temperature smearing causes that the two peaks merge to one already at zero field. Then, again the applied field suppresses the small gap contribution, the peak position first shifts to higher voltages and at a certain field it starts to shrink.

Being aware of possible uncertainty we can define the magnetic field where the shift of the peak towards higher voltages turns back to lower voltages as the "upper critical field" H_{c2} of the π -band without any interband scattering. At 4.2 K this field is at about 1.7 Tesla, at 15 K at about 1.4 T, at 25 K at about 0.7 T. The full temperature dependence of this pair-breaking field of the π -band H_{c2} determined in the same way at more temperatures is displayed in Fig. 6. The obtained temperature dependence reveals a qualitative agreement with the Werthamer, Helfand and Hohenberg prediction for one-band type-II superconductor [35].

Due to the interband scattering, the superconductivity would be present in the π -band also above H_{c2} as induced from the σ -band until the same T_c and the bulk H_{c2} . In this sense H_{c2} would only be a certain crossover field where the small superconducting energy gap gets filled. In our data in the Fig. 5 it is indeed demonstrated that the superconductivity persists well above H_{c2} and is still observable at 3-4 T mainly due to the large energy gap on the π -band.

The effect reveals differently in different experiments. Bouquet et al. [11] have shown in their low temperature specific heat experiments on MgB_2 single crystals that up to 0.5 Tesla the electronic contribution term grows extremely rapidly and isotropically with magnetic field. The effect has been attributed to the filling of the small gap on the π -band. Then, at higher fields an isotropic increase of χ was observed crossing the normal state values at $H_{c2jjc} \approx 3$ T and $H_{c2jjab} \approx 18-22$ T. By scanning tunneling spectroscopy Eskildsen et al. [12] have observed a very large vortex core $\xi = 50$ nm for the magnetic field H_{jjc} corresponding to $H_{c2} = 0.13$ T while the real H_{c2jjc} was again about 3 T.

In recent transport, ac-susceptibility and specific heat measurements on the MgB_2 single crystals [36], we have shown the temperature dependence of the upper critical field for both principal orientations with $H_{c2jjc}(0\text{ K}) \approx 3.5$ T and $H_{c2jjab}(0\text{ K}) \approx 17$ T. In the point-contact measurements shown in Fig. 5 the superconducting feature is getting completely suppressed (i.e. the π -band large gap is suppressed) above 5 T indicating that this particular orientation of the magnetic field with respect to the crystallite under the tip was in between the c -axis and the ab -planes of MgB_2 .

In Fig. 7 a behavior of the Cu-MgB₂ junction with two superconducting energy gaps as a function of the magnetic field is shown. Data are presented for two different contacts (one data set for fields below 3 T and the other for higher fields up to 20 T) with comparable zero-field spectra. The weight parameter α was equal to 0.68 what is in a perfect agreement with the calculations of Brinkman et al. [30] for the important MgB₂ ab-plane current component. The small gap is again suppressed at small fields around 1-2 Tesla but the large gap persists close to H_{c2j_{ab}}. We conclude that while the smaller gap is rapidly closed by a small magnetic field, the large gap is closed at the anisotropic H_{c2}.

Similar conclusions on a rapid closing of the small energy gap in a field of about 1 Tesla and an anisotropic closing of α at much higher fields near the real H_{c2} have been confirmed by the later study of Gonnelli et al. [33].

IV. ELECTRON-PHONON INTERACTION

Ballistic contacts between normal metals have been successfully used for a direct measurement of the electron-phonon interaction [38,39]. For the situation of a long mean-free-path compared to the contact size, the electrons passing the metallic contact are accelerated with a well defined excess energy eV given by the applied voltage over the contact. After an inelastic scattering process (for instance the spontaneous emission of phonons) the injected electrons can flow back through the contact. These inelastic scattering processes lead to corrections to the current which depend on the applied voltage because of the energy-dependent scattering rate of the electrons. Finally, the measured second derivative d^2V/dI^2 is directly proportional to the electron-phonon interaction function α^2F . The Eliashberg function α^2F is the convoluted product of the phonon density of states F and the matrix element α for the electron-phonon interaction. This method has been extensively employed for the investigation of the electron-phonon interaction in normal metals. However, for superconductors the same method can be used by applying a magnetic field to drive the metal into the normal state.

Point-contact studies of the non-linear current-voltage characteristics in the superconducting state have also revealed features of the electron-phonon interaction in the d^2V/dI^2 curves (see for a review [40]). These structures are explained in terms of either the inelastic quasiparticle scattering near the point contact or the energy-dependence of the energy gap. The former mechanism is similar to the point-contact spectroscopy in the normal metals: the quasiparticles generate phonons and are back scattered to the free quasiparticle states, now those available in the superconducting state. The latter mechanism is of importance for strong coupling superconductors. The elastic current channel in the point contact

comprises the excess current due to the Andreev reflection and depends on the superconducting energy gap, analogously to the Rowell-McMillan spectroscopy of the electron-phonon interaction in tunneling experiments. If the spectrum is just due to the second mechanism it cannot be observed above the superconducting phase transition.

A few studies have been devoted on an experimental study of the electron-phonon interaction in MgB₂ using point contacts [14,17]. The measurements of [15] have been done on Nb-MgB₂ (compacted powder) junctions at 4.2 K. The observed nonlinearities in the d^2V/dI^2 (V) characteristics have been interpreted in the framework of the Rowell-McMillan spectroscopy of the electron-phonon interaction in tunneling experiments accounting for the proximity effect. The calculated Eliashberg function reveals three peaks located at 37, 62 and 90-92 meV. The energy position is in agreement with the characteristic phonon energies of MgB₂ as detected by neutron experiments [41,42]. The peak intensity at 62 meV does not show a prevailing amplitude. The calculations of Liu et al. [4] predict a strong anharmonic electron-phonon coupling between the in-plane boron mode E_{2g} near 60 meV and the p_x-y orbitals forming the 2D Fermi sheets, but to resolve this the k-space sensitive experiments on single crystals are necessary.

Figure 8 shows the d^2V/dI^2 spectra of the point contact with significant two gap features. Now the spectra are shown in a voltage (energy) scale up to 120 mV. They were measured below and above the superconducting transition T_c(H) [43]. The top panel shows d^2V/dI^2 curves measured in a fixed magnetic field of 9 Tesla at different temperatures. The bottom panel displays field dependencies of d^2V/dI^2 curves at a fixed temperature of T = 30 K. The dotted lines in both panels represent the spectra in the normal state. At the top curves in the both panels, the observed structure below 10 meV is related to the superconducting energy gap. The d^2V/dI^2 spectra in the normal state show structures centered around 38, 62, 80, and 92 mV. Similar point-contact data have been reported by Bobrov et al. on c-axis oriented MgB₂ thin films [14]. These voltage positions can be well compared with the observed peaks in the phonon density of states obtained from inelastic neutron scattering experiments (acoustic phonon peak at 36 meV, optic bands at 54, 78, 89 and 97 meV [41]). In the point-contact data the E_{2g} mode is more situated around 60 meV instead of around 54 meV from the neutron data. Both experimental techniques show a broadening of up to 10 meV in phonon data which can be partly ascribed to the dispersion of the optic phonon branches.

The calculations of Liu et al. [4] beside a strong anharmonic electron-phonon coupling between the E_{2g} mode and the 2D Fermi sheets, foresee a hardening (12%) of this mode upon entering into the superconducting state. Choi et al. [44] have predicted the dominant peak in the

Eliashberg function $^2F(\omega)$ at 63 meV for the case of harmonic phonons but at 77 meV for anharmonic phonons. We also do not observe a particularly strong one peak in comparison with others in this energy range in the point-contact spectra. Moreover, there is no significant change in position and intensity of the electron-phonon interaction structure upon passing through the superconducting transition [16]. It means that observed structures in our d^2V/dI^2 spectra are not due to the strong coupling effect but rather due to the inelastic scattering.

Following experimental studies of Yanson et al. [17] show similar energy correlations of their $d^2V/dI^2(V)$ spectra with the phonon density of states [45]. Moreover, it is shown that in the point-contact spectra with a small value of the MgB₂ superconducting energy gap (Δ) only a weak structure due to the electron-phonon interaction is observed but the structure grows when is increased to about 3.5 meV presumably due to the interband scattering.

Raman studies have also not observed any hardening of the E_{2g} mode below the superconducting transition temperature [46]. We note that the spectroscopic measurements of the electron-phonon interaction have been done on polycrystals of unknown contact orientation. Like for the case of the energy-gap structure, the contact orientation will also influence the measured electron-phonon interaction spectra via the anisotropy. Therefore, single crystal studies are expected to give further conclusive information with respect to the electron-phonon interaction in MgB₂.

V. CONCLUSIONS

In conclusion, we have demonstrated that the magnesium diboride is a two-gap superconductor. The small gap on the three-dimensional γ -band is very weakly coupled with $2\Delta = k_B T_c \approx 1.7$ and the large gap is strongly coupled with $2\Delta = k_B T_c \approx 4$. The small superconducting energy gap can be suppressed by the magnetic field of about 1-2 Tesla at low temperatures. This field represents the γ -band upper critical magnetic field H_{c2} if there was no interband scattering to the γ -band. Its temperature dependence presented for the first time in this paper, reveals conventional behavior predicted for a one-band type-II superconductor. The large gap along with the anisotropy of the Fermi surface are decisive for the real upper critical field of MgB₂. Superconductivity in MgB₂ is mainly supplied by electrons from the γ -band. Preliminary point-contact experiments on the electron-phonon interaction reveal the phonon modes in the measured second derivatives of the current-voltage characteristics but do not show a particular stronger coupling of the in-plane E_{2g} boron mode. Forthcoming point-contact experiments on single crystals will be very worthwhile to

resolve the problem of the anisotropic electron-phonon interaction.

V I. ACKNOWLEDGMENTS

This work has been supported by the Slovak grant APVT-51-020102, the European Science Foundation ESF - VORTEX programme and the international bilateral programme of cooperation between the CNRS and the Slovak Academy of Sciences.

-
- [1] J. Nagamatsu et al, Nature 410, 63 (2001).
 - [2] H. Suhl, B. T. Matthias, and L. R. Walker, Phys. Rev. Lett. 3, 552 (1959).
 - [3] G. Binnig, A. Barato, H. E. Hoening, and J. C. Bednorz, Phys. Rev. Lett. 45, 1352 (1980).
 - [4] A. Y. Liu, I. I. Mazin, and J. Kortus, Phys. Rev. Lett. 87, 087005 (2001).
 - [5] F. Bouquet et al, Phys. Rev. Lett. 87, 047001 (2001); Y. Wang et al, Physica C 355, 179 (2001).
 - [6] F. Giubileo et al, Phys. Rev. Lett. 87, 177008 (2001).
 - [7] M. Iavarone et al, Phys. Rev. Lett. 89, 187002 (2002).
 - [8] H. Suderow et al, Physica C 369, 106 (2002).
 - [9] X. K. Chen et al, Phys. Rev. Lett. 87, 157002 (2001).
 - [10] P. Szabo et al, Phys. Rev. Lett. 87, 137005 (2001).
 - [11] F. Bouquet et al, cond-mat/0207141.
 - [12] M. R. Eskildsen et al, Phys. Rev. Lett. 89, 187003.
 - [13] E. A. Yelland et al, Phys. Rev. Lett. 88, 217002 (2002).
 - [14] N. L. Bobrov et al, in New Trends in Superconductivity, eds. J. F. Annett and S. K. Krichin, Kluwer Academic Publishers, Dordrecht 2002, NATO Science Series II: Mathematics, Physics and Chemistry, Vol. 67, p. 225.
 - [15] A. I. D'yachenko et al, cond-mat/0201200.
 - [16] P. Szabo, P. Samuely, J. Kacmarcik, T. Klein, J. M. Arcus, and A. G. M. Jansen, to appear in Physica C.
 - [17] I. K. Yanson et al, cond-mat/0206170.
 - [18] K. Mullen, E. Ben-Jacob and S. Ruggiero, Phys. Rev. B 38, 5150 (1988).
 - [19] G. E. Blonder, M. Tinkham, and T. M. Klapwijk, Phys. Rev. B 25, 4515 (1982).
 - [20] A. Plecenik et al, Phys. Rev. B 49, 10016 (1996).
 - [21] H. Schmidt, J. F. Zasadzinski, K. E. Gray, and D. G. Hinks, Phys. Rev. B 63, 220504 (2001).
 - [22] A. Kohnen and G. Detscher, Phys. Rev. B 64, 060506 (R) (2001).
 - [23] J. Kortus et al, Phys. Rev. Lett. 86, 4656 (2001).
 - [24] A. Plecenik, S. Benacka, P. Kus, and M. G. Rajcar, Physica C 386, 251 (2002).
 - [25] F. Laube et al, Europhys. Lett. 56, 296 (2001).
 - [26] R. S. Gonnelli et al, Int. J. Mod. Phys. 16, 1553 (2002).
 - [27] S. Lee et al, Physica C 377, 202 (2002).
 - [28] Z.-Z. Li et al, Phys. Rev. B 66, 064513 (2002).
 - [29] P. Szabo, P. Samuely, J. Kacmarcik, T. Klein, J. M. Arcus, A. G. M. Jansen, to appear in Physica B (2003).

- [30] A. Brinkman et al, Phys. Rev. B 65, 180517(R) (2001).
- [31] Y. Bugoslavsky et al, Supercond. Sci. Technol. 15, 526 (2002).
- [32] Yu. G. Naidyuk et al, JETP Letter 75, 238 (2002).
- [33] R. S. Gonnelli et al, cond-m at/0208060.
- [34] P. Szabo et al, J. Low Temp. Phys. 106, 291 (1997); P. Szabo, P. Samuely, A. G. M. Jansen, J. Marcus, P. Wyder, Phys. Rev. B 62, 3502 (2000).
- [35] N. R. Werthamer, E. Helfand, and P. Hohenberg, Phys. Rev. 147, 295 (1966).
- [36] L. Lyard et al, to appear in Phys. Rev. B (2002); cond-m at/0206231.
- [37] P. Szabo et al, to appear in Supercond. Sci. Technol.
- [38] I. K. Yanson, Zh. Eksp. Teor. Fiz. 66, 1035 (1974) [Sov. Phys. - JETP 39, 506 (1974)].
- [39] A. G. M. Jansen, A. P. van Gelder, and P. Wyder, J. Phys. C: Solid State Phys. 13, 6073 (1980).
- [40] I. K. Yanson, in Quantum Mesoscopic Phenomena and Mesoscopic Devices in Microelectronics, eds. I. O. Kulik and R. Ellialtıoglu, Kluwer Academic Publishers, 2000, p.61.
- [41] R. Osborn et al, Phys. Rev. Lett. 87, 017005 (2001).
- [42] T. Yildirim et al, Phys. Rev. Lett. 87, 037001 (2001).
- [43] P. Szabo et al, Physica C 369, 250 (2002).
- [44] H. J. Choi, D. Roundy, H. Sun, M. L. Cohen, and S. G. Louie, Phys. Rev. B 66, 020513 (R) (2002).
- [45] B. Renker et al, Phys. Rev. Lett. 88, 067001 (2002).
- [46] H. M. artinho et al, cond-m at/0105204.

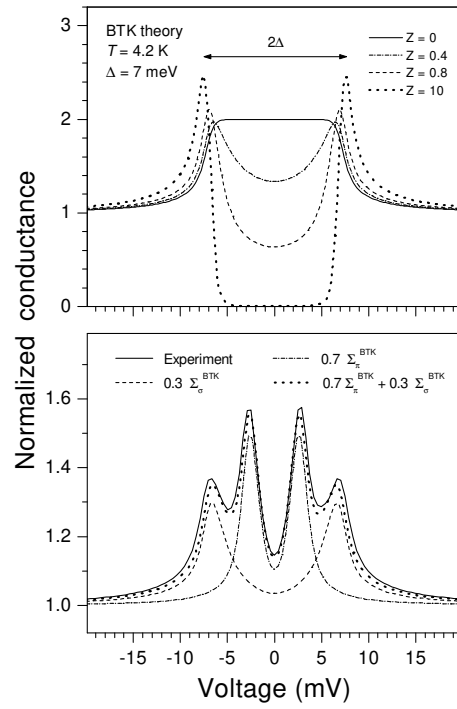


FIG. 1. a) Numerical simulation of the BTK model at different values of the barrier strength Z , representing behavior of the point-contact spectra for $\Delta = 7$ meV between Giaever tunneling ($Z = 10$) and clean Andreev reflection ($Z = 0$) at $T = 4.2$ K [10]. b) The Andreev reflection spectrum with two gaps on the Cu-MgB₂ junction together with fitting by two BTK conductances (0.3 Σ_e^{BTK} and 0.7 Σ_e^{BTK} curves are shifted to unity). The final fitting curve has been generated at $Z = 0.5$, $\Delta = 2.8$ meV, $\Delta = 7$ meV, $\Delta = 0$ with a weight = 0.7 at $T = 4.2$ K [29].

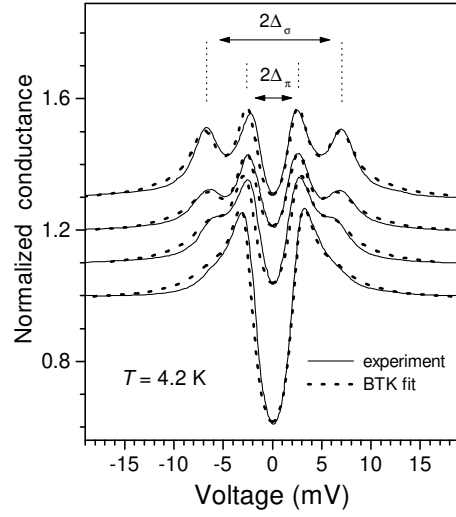


FIG . 2. b) Cu -M gB₂ point-contact spectra at T = 4.2 K (full lines). The upper curves are vertically shifted for the clarity. Dotted lines display fitting results for the thermally smeared BTK model with $\Gamma = 2.8 \pm 0.1$ m eV, $\Delta = 6.8 \pm 0.3$ m eV for different barrier transparencies and weight factors [10].

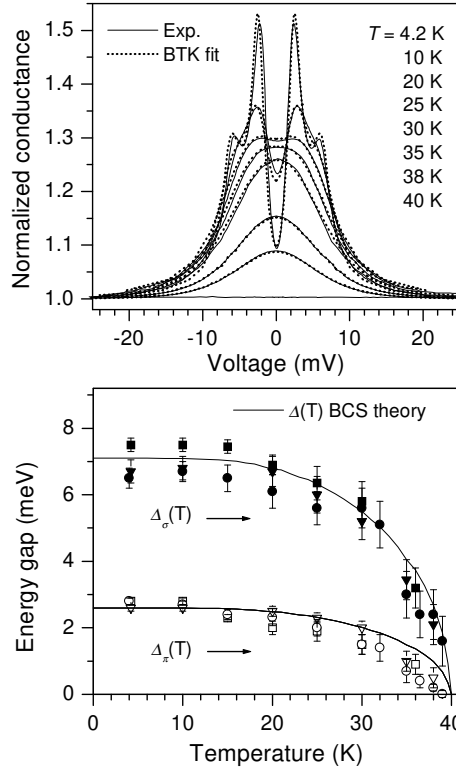


FIG . 3. a) Differential conductances of Cu -M gB₂ point-contact measured (full lines) and fitted (dotted lines) for the thermally smeared BTK model at indicated temperatures. The fitting parameters $\Gamma = 0.71$, $Z = 0.52 \pm 0.02$, $\Delta = 0.02$ m eV had the same values at all temperatures. b) Temperature dependencies of both energy gaps ($\Delta_{\sigma}(T)$ - solid symbols, $\Delta_{\pi}(T)$ - open symbols) determined from the fitting on three different point-contacts are displayed with three corresponding different symbols. $\Delta_{\sigma}(T)$ and $\Delta_{\pi}(T)$ points determined from the same contact are plotted with the same (open and solid) symbols. Full lines represent BCS predictions [10].

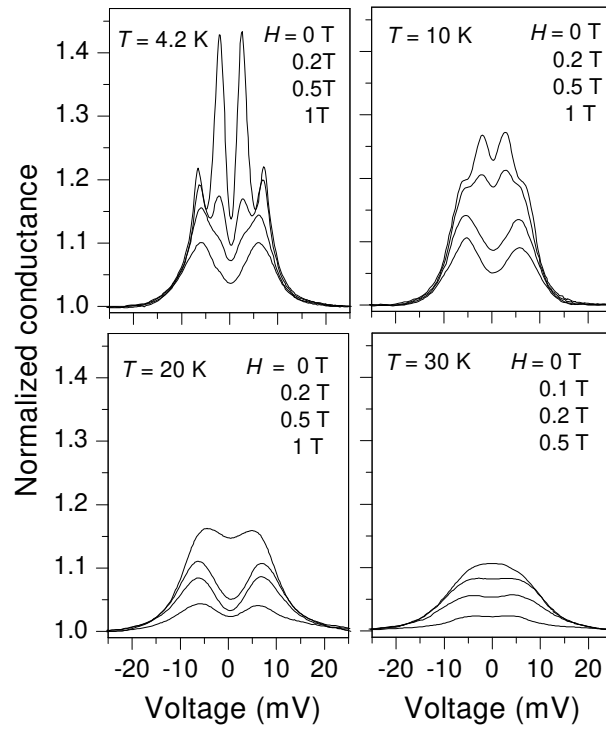


FIG. 4. Experimentally observed influence of the applied magnetic field on the two-gap structure of the normalized point-contact spectra at indicated temperatures. These spectra clearly reveal that both gaps exist in zero field up to T_c as shown by the rapid suppression of the small gap structure ($\Delta = 2.8 \text{ meV}$) with magnetic field which leads to a broad deep minimum at zero bias [10].

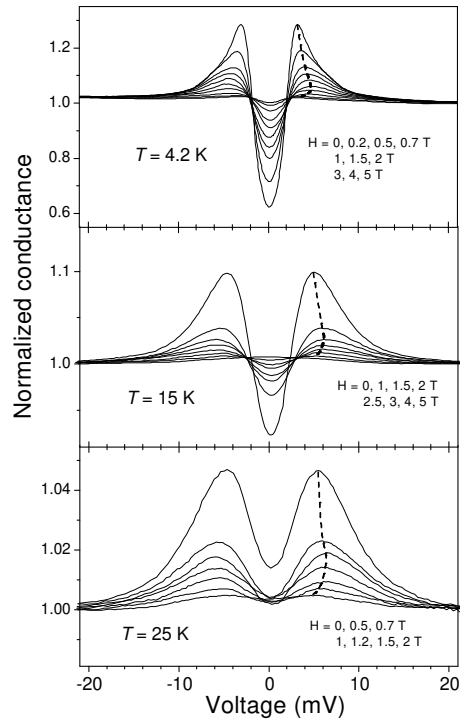


FIG. 5. On-gap spectrum of the Cu-MgB₂ junction with the c-axis current injection at 4.2 K, 15 K and 25 K in different magnetic fields. The dashed lines show evolution of the peak position in magnetic field. The maximal value of this voltage position is a measure of the critical field for the suppression of the small gap.

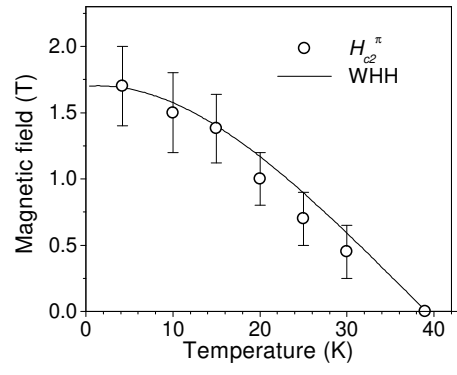


FIG . 6. Temperature dependence of the c_2 -band pair-breaking magnetic field $H_{c_2}^\pi$

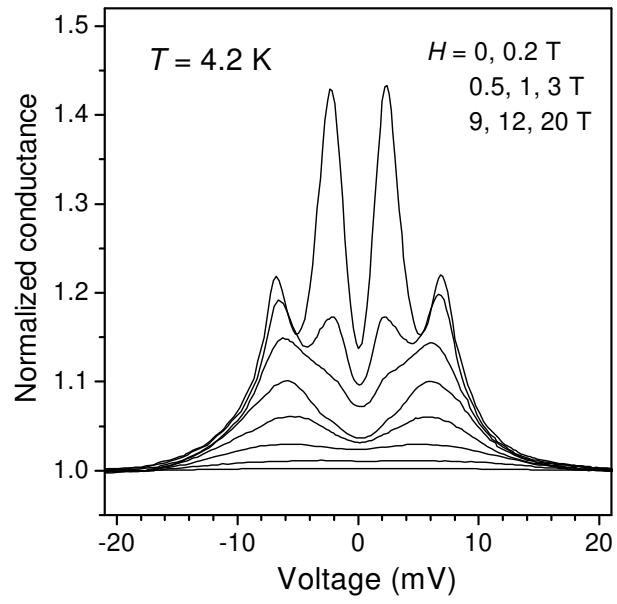


FIG. 7. Cu-MgB₂ point-contact spectrum showing two gaps with an important ab-plane current contribution in fields approximately parallel to the ab-planes of MgB₂ up to 20 T at 4.2 K [37].

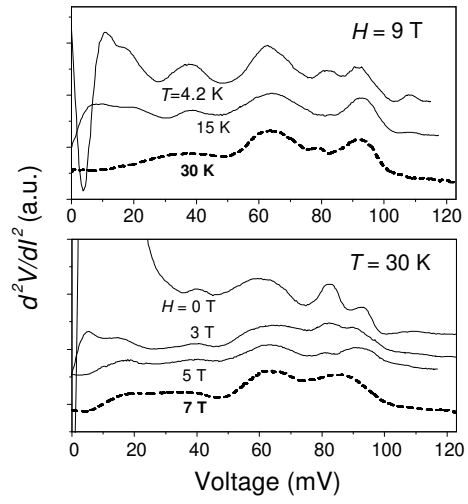


FIG. 8. Point-contact spectra d^2V/dI^2 (V) of the Cu-MgB₂ junction measured at different temperatures and magnetic fields below and above the superconducting transition (dashed lines in the normal state) [16].